PHYSICAL REVIEW B VOLUME 56, NUMBER 15 15 OCTOBER 1997-I

Interstitial oxygen in silicon under hydrostatic pressure

M. D. McCluskey and E. E. Haller
Lawrence Berkeley National Laboratory and University of California, Berkeley, California 94720

(Received 13 May 1997)

Using infrared spectroscopy, we have measured the vibrational spectrum of interstitial oxygen in silicon under hydrostatic pressures as high as 70 kbar at temperatures from 4 to 20 K. The application of pressure transforms the transverse motion of the oxygen from that of a harmonic oscillator to that of a rotor. As the motion becomes more rotational, the splitting between the $l=0$ and $l=\pm 1$ low-frequency modes decreases. In addition, the splitting between the stretch modes at 1136 and 1128 cm^{-1} decreases with increasing pressure and can no longer be resolved for pressures greater than 55 kbar. [S0163-1829(97)06140-7]

Oxygen is an omnipresent, technologically important impurity in Czochralski-grown Si.[1] The theories of the diffusion[2,3] and vibrational motion[4] of oxygen in Si are currently active areas of research. In as-grown Si crystals, oxygen exists primarily as an interstitial defect, denoted O_i.[5,6] In this form, the oxygen binds with two Si atoms, residing in an off-center position in the [111] plane equidistant from the Si atoms. Using local vibrational mode spectroscopy,[7,8] Hrostowski and Kaiser[9] measured the now-famous 1136 cm^{-1} absorption peak of the $^{16}\mathrm{O}_i$ stretch mode at liquid-helium temperatures. Pajot[1] measured the stretch-mode frequencies of the isotopes $^{17}\mathrm{O}_i$ and $^{18}\mathrm{O}_i$ at 1107 and 1084 cm^{-1}, respectively. These values are in good agreement with a simple harmonic-oscillator model in which the vibrational frequency is inversely proportional to the square root of the oxygen mass. The stretch mode is an oscillation of the O_i atom along the [111] direction, out of phase with the two nearest Si atoms. In the X-Y-X model of nonlinear molecules,[10] the stretch mode is denoted ν_3, while the off-axis modes are denoted ν_1 and ν_2. Different isotopic combinations of Si atoms lead to a well-explained splitting of a few cm^{-1}, lending further support to the Si-O-Si model.[11]

In addition to the stretch mode, O_i has low-frequency modes in the [111] plane perpendicular to the Si$\cdots$Si broken bond. Bosomworth *et al.*[12] measured a low-frequency vibration at 29 cm^{-1} at a temperature of 2 K. As the temperature is raised, the excited low-frequency states become thermally populated, resulting in a splitting of the stretch-mode peak. The O_i state is denoted $|k,l,N\rangle$, where k is the radial quantum number, l is the angular momentum about the [111] axis, and N is the longitudinal- (stretch) quantum number. At atmospheric pressure and a temperature of 20 K, the $|0,0,0\rangle \rightarrow |0,0,1\rangle$ and $|0,\pm 1,0\rangle \rightarrow |0,\pm 1,1\rangle$ transitions yield the well-known absorption peaks at 1136 and 1128 cm^{-1}, respectively. We have measured the dependence of these stretch-mode peaks on hydrostatic pressure.

We used a modified Merill-Bassett diamond-anvil cell[13,14] with type-II A diamonds to generate pressures up to 70 kbar. The Si samples were cut into disks 300 μm in diameter and polished to a thickness of 50 μm. Nitrogen was used as a pressure medium and was loaded into the cell, along with the sample, using the liquid-immersion technique.[15] To determine the pressure at liquid-helium temperatures, we measured the infrared-absorption peak of the ν_3 vibrational mode of CO_2 impurities in the N_2 matrix. The ν_3 mode varies linearly with pressure[16] and provides a precise *in situ* calibration of the pressure.

Mid-infrared absorption spectra were obtained with a Digilab FTS-80E vacuum Fourier-transform spectrometer with a KBr beam splitter and a spectral range of 450–3400 cm^{-1}. The Si:O samples were kept at temperatures ranging from 4 to 20 K in a Janis liquid-helium cryostat with KBr windows. The instrumental resolution was varied from 0.5 to 1 cm^{-1}, such that all the peaks were fully resolved. A light-concentrating cone focused the light through the diamonds, the sample, and into a Ge:Cu photoconductor mounted directly behind the sample. The Si:O samples were Czochralski-grown with an oxygen concentration of $9 \times 10^{17}\ \mathrm{cm}^{-3}$.

In our experiment, we measured the $|0,0,0\rangle \rightarrow |0,0,1\rangle$ and $|0,\pm 1,0\rangle \rightarrow |0,\pm 1,1\rangle$ transitions, denoted I and II, respectively, as a function of hydrostatic pressure at a temperature of 9 K (Fig. 1). As the pressure increases from atmospheric pressure, the area of peak II increases at the expense of peak I. This behavior can be explained by a pressure-dependent

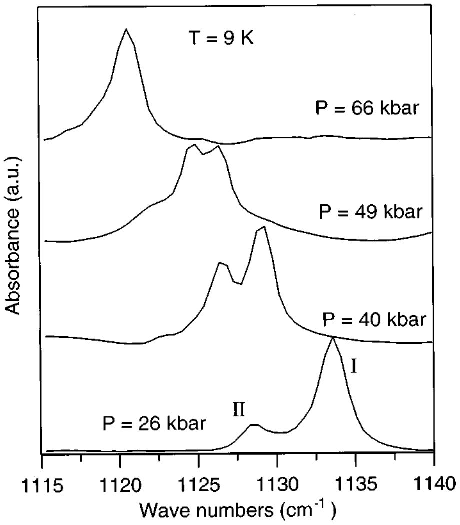

FIG. 1. Pressure dependence of stretch-mode absorption peaks in Si:O at a temperature of 9 K. Peaks I and II correspond to the $|0,0,0\rangle \rightarrow |0,0,1\rangle$ and $|0,\pm 1,0\rangle \rightarrow |0,\pm 1,1\rangle$ transitions, respectively.

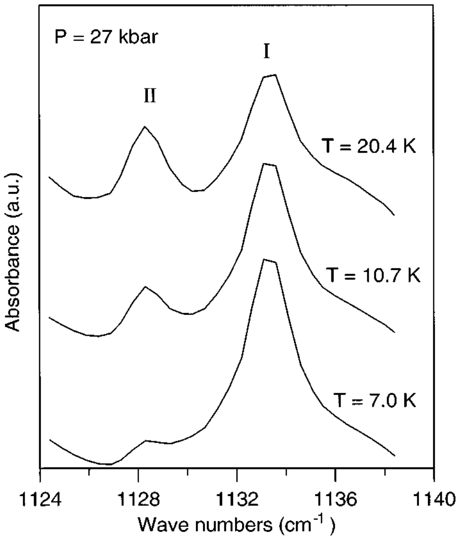

FIG. 2. Temperature dependence of stretch-mode absorption peaks in Si:O at a pressure of 27 kbar. Peaks I and II correspond to the $|0,0,0\rangle \rightarrow |0,0,1\rangle$ and $|0,\pm 1,0\rangle \rightarrow |0,\pm 1,1\rangle$ transitions, respectively.

decrease in the energy difference between the $|0,0,0\rangle$ and $|0,\pm 1,0\rangle$ ground states. As the ground-state splitting decreases, the higher-energy $|0,\pm 1,0\rangle$ state becomes thermally more populated, leading to an increase in the area of peak II. To experimentally determine the ground-state splitting, we measured the areas of peaks I and II as a function of temperature for some of the pressures (Fig. 2). The ratio of the areas is graphed in an Arrhenius plot to obtain an activation energy, with an uncertainty of ± 2 cm^{-1} estimated by varying the slope of the linear fit. This activation energy is due to the ground-state splitting and is plotted as a function of pressure in Fig. 3. It is clear that the ground-state splitting decreases as the pressure increases.

In addition to reducing the splitting of the ground state, the application of pressure also decreases the frequency difference between the I and II absorption peaks. The frequencies of the peaks are plotted as a function of pressure in Fig. 4. Beyond 55 kbar, the splitting can no longer be resolved, as the two peaks effectively merge. These observations can be explained by considering that as pressure is applied, the Si atoms exert a force on the O_i atom, causing it to buckle outward. As the radial distance of the O_i atom increases, the potential in the [111] plane transforms from a perturbed harmonic oscillator to a rotor. This model is discussed in the following paragraphs.

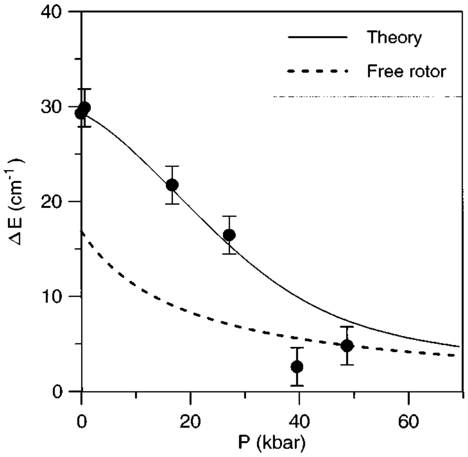

FIG. 3. Pressure dependence of the split between the $|0,0,0\rangle$ and $|0,\pm 1,0\rangle$ ground states. The solid line is a plot of the theory [Eqs. (2)–(7)] and the dashed line is the splitting for a free rotor [Eq. (8)].

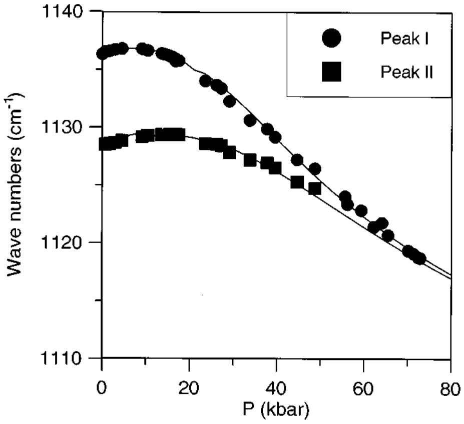

FIG. 4. Plot of the stretch-mode frequencies in Si:O as a function of pressure at a temperature of 9 K. The solid lines are plots of the theory [Eqs. (9)–(13)].

To quantitatively explain the low-frequency modes, Yamada-Kaneta, Kaneta, and Ogawa[17] described the O_i potential in the [111] plane as a quartic polynomial:

$$V(r)=\tfrac{1}{8}m\omega_0^2(r^4/r_0^2-2r^2), \tag{1}$$

where r is the perpendicular distance from the Si···Si broken bond, r_0 is the equilibrium distance, and ω_0 is the classical vibrational frequency at r_0. With an appropriate choice of parameters, Eq. (1) approximates a parabolic potential with a central perturbation. By adjusting the parameters to fit the experimental data, Yamada-Kaneta, Kaneta, and Ogawa[17] derived a value of $r_0=0.25$ Å for the ground state, in agreement with Bosomworth *et al.*[12]

To calculate the wave functions in the [111] plane, we numerically solve Schrödinger's equation. Assuming cylindrical symmetry, the radial part of Schrödinger's equation is given by

$$-\frac{\hbar^2}{2m}\left[\frac{1}{r}\frac{\partial}{\partial r}\left(r\frac{\partial}{\partial r}\right)+\frac{1}{r^2}\frac{\partial^2}{\partial\theta^2}\right]\psi_{k,l}(r)+V(r)\psi_{k,l}(r)$$
$$=E\psi_{k,l}(r), \tag{2}$$

where m is the mass of ^{16}O, $V(r)$ is given in Eq. (1), l is the angular momentum about the [111] axis, and k is the radial quantum number. As the potential only depends on r, the wave function can be expressed as the product of a radial and an angular function,

$$\psi_{k,l}(r)=u_l(r)e^{il\theta}. \tag{3}$$

Since $k=0$ in the states of interest, we have dropped the k subscript. Substituting Eq. (3) into Eq. (2) yields

TABLE I. Parameters used in the theoretical model [Eqs. (6)–(13)].

Parameter	Value
a	1.02×10^{-3} Å/kbar
b	300 cm^{-1}/Å
α'	218 $\text{cm}^{-1}/\text{Å}^{2}$
β'	133 $\text{cm}^{-1}/\text{Å}^{4}$
ω_{s0}	1150.6 cm^{-1}
γ	0.23 cm^{-1}/kbar

$$-\frac{\hbar^2}{2m}\left[\frac{1}{r}\frac{d}{dr}\left(r\frac{d}{dr}\right)+\frac{l^2}{r^2}\right]u_l(r)+V(r)u_l(r)=Eu_l(r). \tag{4}$$

We numerically integrate Eq. (4) from $r=0-3$ Å with a step size of 6×10^{-4} Å and an initial energy eigenvalue of $E=10\ \text{cm}^{-1}$. The eigenvalue E is varied until the wave function converges to zero at $r=3$ Å. For the $l=0$ state, the initial conditions are given by $u_0=1$ and $du_0/dr=0$. For the $l=\pm1$ states, the initial conditions are $u_{\pm1}=0$ and $du_{\pm1}/dr=1$.

The equilibrium radial distance is given by

$$r_0^2=d_{\text{Si-O}}^2-z_{\text{Si}}^2, \tag{5}$$

where z_{Si} is the perpendicular distance of the Si atoms from the [111] plane of the O_i, given by

$$z_{\text{Si}}(P)=z_{\text{Si}}(0)-aP, \tag{6}$$

and $d_{\text{Si-O}}$ is the Si-O bond length (1.6 Å), assumed to have a pressure dependence that is negligible compared to that of z_{Si}. Following the results of Ref. 17, $z_{\text{Si}}(0)$ is chosen to yield a value of $r_0=0.25$ Å at zero pressure. For simplicity, the value of ω_0 in Eq. (1) is assumed to vary linearly with r_0:

$$\omega_0=44\ \text{cm}^{-1}+b(r_0-0.25\ \text{Å}). \tag{7}$$

The parameters that give the best fit to the experimental data are listed in Table I.

The calculated wave functions are shown in Fig. 5 for 0 and 60 kbar. As the pressure increases, the height of the central perturbation increases and the $l=0$ and $l=\pm1$ radial wave functions become more similar. The theoretical ground-state splitting is plotted as a function of pressure in Fig. 3 and shows reasonable agreement with the experimental data. As the central perturbation grows, the O_i transverse motion becomes less vibrational and more rotational. A free rotor has an energy splitting given by

$$\Delta E_{\text{ROT}}\equiv E(l=1)-E(l=0)=\frac{\hbar^2}{2mr_0^2}. \tag{8}$$

As shown in Fig. 3, the theoretical ground-state splitting approaches that of a rotor as pressure increases. For pressures greater than 30 kbar, the experimental splittings are lower than the theoretical values, perhaps due to neighboring Si atoms hindering the rotational motion as the O_i buckles outward. In the following paragraphs, we use the same model to explain the pressure dependence of the peak frequencies. It is interesting to note that in Ge, O_i is significantly displaced off-axis and acts as a hindered rotor at atmospheric pressure.[18,19] In Si we have used hydrostatic pressure to *force* O_i into an off-axis configuration.

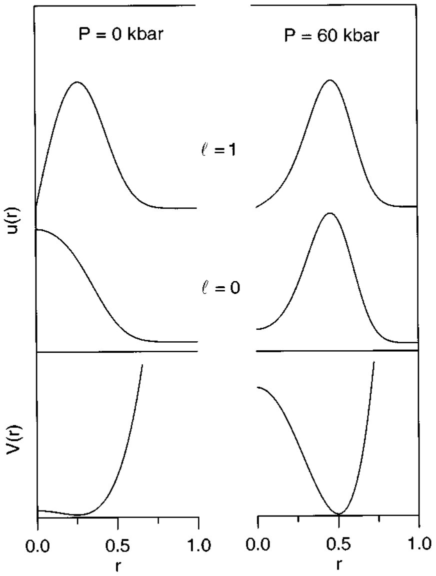

FIG. 5. Theoretical potentials $V(r)$ and radial wave functions $u(r)$ of O_i for hydrostatic pressures of 0 and 60 kbar. As the pressure increases, the central bump of the potential grows, pushing the O_i radially outward and making the $l=0$ and $l=1$ wave functions more similar. This model accounts for the observed decrease in the splitting of the ground-state and stretch-mode peaks.

This transition to rotational motion can also explain the merging of the stretch mode peaks. The splitting of peaks I and II is due to nonlinear coupling between the stretch- and low-frequency transverse modes. The lowest-order stretch-transverse coupling term is given by

$$H'=z^2(\alpha r^2+\beta r^4), \tag{9}$$

where z is the coordinate along the [111] axis. To first order, this term perturbs the $N=0\rightarrow N=1$ stretch mode transition by an amount

$$\begin{aligned}\delta\omega_l&=(\langle N=1|z^2|N=1\rangle-\langle N=0|z^2|N=0\rangle)\langle l|\alpha r^2+\beta r^4|l\rangle\\&\equiv-\alpha'\langle r^2\rangle_l+\beta'\langle r^4\rangle_l.\end{aligned} \tag{10}$$

The stretch mode is perturbed by different amounts for $l=0$ and $l=\pm1$, resulting in an energy difference between peaks I and II. As the pressure is increased and the $l=0$ and $l=\pm1$ radial wave functions become more similar, this splitting approaches zero.

The final pressure-dependent effect is a slight increase in the stretch-mode frequency as the Si-O bonds are compressed. Because the effect is small, we assume a linear dependence on pressure:

$$\omega_s=\omega_{s0}+\gamma P, \tag{11}$$

where ω_s is the stretch-mode frequency in cm^{-1}. Combining Eqs. (10) and (11) yields

$$\omega_{\text{I}}=\omega_{s0}+\gamma P-\alpha'\langle r^2\rangle_{l=0}+\beta'\langle r^4\rangle_{l=0}, \tag{12}$$

$$\omega_{\text{II}}=\omega_{s0}+\gamma P-\alpha'\langle r^2\rangle_{l=\pm1}+\beta'\langle r^4\rangle_{l=\pm1}, \tag{13}$$

where ω_{I} and ω_{II} are the frequencies of peaks I and II, respectively. The parameters that yield the best fit to the experimental data are listed in Table I. The theoretical expressions [Eqs. (12) and (13)] are plotted in Fig. 4 and show good agreement with the data. As the O_i motion becomes more rotational, the splitting of the peaks decreases until it cannot be resolved for pressures greater than 55 kbar. This is analogous to the case in Ge, where the O_i motion is primarily rotational and the splitting between the I and II peaks is extremely small ($0.07\ \mathrm{cm}^{-1}$).[19]

In conclusion, we have used hydrostatic pressure to probe the vibrational spectrum of Si:O_i. As the pressure increases, the O_i buckles outward and the nature of its transverse motion changes from vibrational to rotational. This transformation from a perturbed harmonic oscillator to a rotor has two consequences. First, the energy difference between the $l=0$ and $l=\pm 1$ states is reduced as the radial wave functions become more similar. Second, the splitting between the $|0,0,0\rangle \rightarrow |0,0,1\rangle$ and $|0,\pm 1,0\rangle \rightarrow |0,\pm 1,1\rangle$ transitions approaches zero. In effect, we have used hydrostatic pressure to simulate the situation in Ge, in which the O_i atom resides in an off-axis location and behaves like a hindered rotor. In the future, hydrostatic pressure may be used to tune the vibrational and rotational modes of impurities and native defects in other semiconductors.

We would like to thank S. McHugo for supplying the Si:O samples and L. Hsu for his assistance with the high-pressure work. We acknowledge the use of facilities at Lawrence Berkeley National Laboratory (LBNL). This work was supported by USNSF Grant No. DMR-94 17763.

---

[1] B. Pajot, in *Semiconductors and Semimetals*, edited by F. Shimura (Academic, New York, 1994), Vol. 42 Chap. 6.

[2] M. Ramamoorthy and S. T. Pantelides, Phys. Rev. Lett. **76**, 267 (1996).

[3] Z. Jiang and R. A. Brown, Phys. Rev. Lett. **74**, 2046 (1995).

[4] E. Artacho, F. Ynduráin, B. Pajot, R. Ramírez, C. P. Herrero, L. I. Khirunenko, K. M. Itoh, and E. E. Haller, Phys. Rev. B **56**, 3820 (1997).

[5] L. Jastrzebski, P. Zanzucchi, D. Thebault, and J. Lagowski, J. Electrochem. Soc. **129**, 1638 (1982).

[6] B. Pajot, H. J. Stein, B. Cales, and C. Naud, J. Electrochem. Soc. **132**, 3034 (1985).

[7] R. C. Newman, *Infrared Studies of Crystal Defects* (Taylor & Francis, London, 1973).

[8] E. E. Haller, in *Defect and Impurity Engineered Semiconductors and Devices*, edited by S. Ashok, J. Chevallier, I. Akasaki, N. M. Johnson, and B. L. Sopori, MRS Symposia Proceedings No. 378 (Materials Research Society, Pittsburgh, 1995), p. 547.

[9] H. J. Hrostowski and R. H. Kaiser, Phys. Rev. **107**, 966 (1957).

[10] G. Herzberg, *Infrared and Raman Spectra of Diatomic Molecules* (Van Nostrand, Princeton, 1945), p. 104.

[11] B. Pajot and J. P. Deltour, Infrared Phys. **7**, 195 (1967).

[12] D. R. Bosomworth, W. Hayes, A. R. L. Spray, and G. D. Watikins, Proc. R. Soc. London, Ser. A **317**, 133 (1970).

[13] L. Merill and W. A. Bassett, Rev. Sci. Instrum. **45**, 290 (1974).

[14] E. Sterer, M. P. Pasternak, and R. D. Taylor, Rev. Sci. Instrum. **61**, 1117 (1990).

[15] D. Schiferl, D. T. Cromer, and R. L. Mills, High Temp.-High Press. **10**, 493 (1978).

[16] M. D. McCluskey, L. Hsu, L. Wang, and E. E. Haller, Phys. Rev. B **54**, 8962 (1996).

[17] H. Yamada-Kaneta, C. Kaneta, and T. Ogawa, Phys. Rev. B **42**, 9650 (1990).

[18] M. Gienger, M. Glaser, and K. Laβmann, Solid State Commun. **86**, 285 (1993).

[19] A. J. Mayur, M. D. Sciacca, M. K. Udo, A. K. Ramdas, K. Itoh, J. Wolk, and E. E. Haller, Phys. Rev. B **49**, 16 293 (1994).